

# Feasibility of Therapeutic Ultrasound Application in Topical Scleral Delivery of Avastin

Hanaa H. Almogbil<sup>1</sup>, Fadi P. Nasrallah<sup>2</sup>, and Vesna Zderic<sup>1</sup>

<sup>1</sup> Department of Biomedical Engineering, The George Washington University, Washington, DC, USA

<sup>2</sup> Retina Consultants, Washington, DC, USA

**Correspondence:** Vesna Zderic, Department of Biomedical Engineering, School of Engineering and Applied Science, The George Washington University, 800 22nd Street NW, rm 6670, Washington, DC 20052, USA.  
e-mail: [zderic@gwu.edu](mailto:zderic@gwu.edu)

**Received:** August 19, 2021

**Accepted:** November 2, 2021

**Published:** December 1, 2021

**Keywords:** anti-VEGF; bevacizumab; sclera; drug delivery; diabetic retinopathy; intravitreal injection; macromolecules; eye drug delivery

**Citation:** Almogbil HH, Nasrallah FP, Zderic V. Feasibility of therapeutic ultrasound application in topical scleral delivery of avastin. *Transl Vis Sci Technol.* 2021;10(14):2, <https://doi.org/10.1167/tvst.10.14.2>

**Purpose:** Macromolecules have been shown to be effective in vision-saving treatments for various ocular diseases, such as age-related macular degeneration and diabetic retinopathy. The current delivery of macromolecules requires frequent intraocular injections and carries a risk of serious adverse effects.

**Methods:** We tested the application of therapeutic ultrasound as a minimally invasive approach for the delivery of Avastin into the diseased regions of the eye. Avastin (bevacizumab) is an anti-vascular endothelial growth factor (VEGF) antibody with a molecular weight of 149 kDa. We tested the effectiveness and safety of Avastin delivery through rabbit sclera in vitro using a standard diffusion cell model. Ultrasound at frequencies of 400 kHz or 3 MHz with an intensity of 1 W/cm<sup>2</sup> was applied for the first 5 minutes of 1-hour drug exposure. Sham treatments mimicked the ultrasound treatments, but ultrasound was not turned on. Absorbance measurements of the receiver compartment solution were performed at 280 nm using a spectrophotometer.

**Results:** Absorbance measurements indicated no statistical difference between the sham ( $n = 13$ ) and 400 kHz ultrasound group ( $n = 15$ ) in the delivery of Avastin through the sclera. However, the absorbance values were statistically different ( $P < 0.01$ ) between the 3 MHz ultrasound group ( $0.004$ ,  $n = 8$ ) and the matched sham group ( $0.002$ ,  $n = 7$ ). There was 2.3 times increase in drug delivery in the 3 MHz ultrasound when compared to the corresponding sham group. Histological studies indicated no significant damage in the ultrasound-treated sclera due to ultrasound application.

**Conclusions:** Our preliminary results provided support that therapeutic ultrasound may be effective in the delivery of Avastin through the sclera.

**Translational Relevance:** Our study offers clinical potential for a minimally invasive retinopathy treatment.

## Introduction

Ocular drugs are delivered through various systemic, topical, subconjunctival, intravitreal, and intrascleral methods.<sup>1-4</sup> The unique structural differences of tissues in the sclera, conjunctiva, and retina block penetration by infectious microorganisms, however, also inhibit ocular delivery of macromolecules.<sup>5,6</sup> Sclera's large surface area and high permeability offers a preferred route for transscleral delivery of macromolecules to the posterior segment of the eye.<sup>7-9</sup> Scleral permeability is affected by the macromolecule weight, radius, and charge.<sup>7,10</sup> The

permeability of the sclera is inversely proportional to the positively charged molecules, molecular weight, and radius.<sup>11,12</sup> Macromolecules have been shown to be effective in vision-saving treatments for various posterior segment ocular diseases, such as age-related macular degeneration and diabetic retinopathy.<sup>4,13</sup> Topical administration is a preferred noninvasive route for application of ophthalmic drugs; however, macromolecules typically cannot penetrate to the posterior segment because of their large size.<sup>14,15</sup> Topical drug administrations showed <5% deeper eye tissues penetration.<sup>14,16</sup> Overall, macromolecules show substantially less penetration through the sclera than smaller molecules.<sup>12</sup> The clinical problem that still

needs to be addressed is maximizing the bioavailability of the administered drug while minimizing the eye barrier resistance.

Bevacizumab (commercial name Avastin; with a molecular weight of 149 kDa) is a recombinant humanized IgG1 monoclonal antibody that inhibits angiogenesis by binding with high affinity to human vascular endothelial growth factor (VEGF).<sup>17</sup> Avastin, an anti-VEGF antibody, is being used against different types of cancer and has also been successfully used in ophthalmology, although off-label, for the treatment of diseases such as diabetic retinopathy, age-related macular degeneration (wet form), neovascular glaucoma, and several other conditions characterized by neovascularization.<sup>17,18</sup> Steroid injections, laser treatment, and anti-VEGF agents are currently used therapies for most retinal diseases and are selected based on the clinical scenario.<sup>19</sup> The most common route of delivering the macromolecules to the posterior segment requires frequent intravitreal injections that carry a risk of serious adverse effects.<sup>13,14</sup> Intravitreal injection of anti-VEGF requires a monthly injection, which can lead to patient discomfort, increase chance of postinjection infections, and related complications.<sup>20–22</sup> Steroids implants, such as intravitreal triamcinolone (IVTA), Dexamethasone (DEX), and fluocinolone acetonide (FA), are all effective in the treatment of retinal vascular diseases.<sup>19</sup> DEX implants are also effective for the treatment of diabetic retinopathy as an alternative and/or in combination with anti-VEGF therapy.<sup>23–27</sup> Previous studies have shown that DEX intravitreal implants can deliver a sustainable release of macromolecules into the eye, which can help control the severity of diabetic macular edema (DME) and complications after vitrectomy surgery.<sup>23–27</sup> Moreover, eyes that were nonresponsive to anti-VEGF medication were shown to have better results when DEX implants were used.<sup>28</sup> Laser therapies have become a second-line therapy when patients have poorly controlled glaucoma or fail to respond to steroid therapies.<sup>19</sup> These methods can be invasive and often require long-term repeated therapy.<sup>1–4,29</sup> Furthermore, they may present a significant financial and time-consuming burden on both the patients and the medical system.<sup>5,14,29,30</sup> A study conducted on 314 patients undergoing anti-VEGF therapy showed that the most common reason leading to noncompliance was the fear of the therapy.<sup>31</sup> Therefore, a noninvasive delivery method for macromolecules is needed for the treatment of eye diseases.<sup>4</sup>

Therapeutic ultrasound offers a noninvasive delivery potential to enhance ocular delivery.<sup>32,33</sup> Anti-VEGF injection is associated with vision improvement;

however, ophthalmologists have recognized the burden of poor patient compliance and tolerance of the monthly regular visit for the injection treatment.<sup>30,34</sup> An ultrasound approach for the delivery of anti-VEGF drugs may lead to improved patient outcomes in terms of higher treatment compliance and avoidance of side effects associated with injection treatment.<sup>31</sup> Our previous research findings indicated that ultrasound can be effective and safe for transcorneal delivery of various topically applied compounds into the eye, including the small hydrophilic drug-mimicking compound sodium fluorescein, steroid DEX sodium phosphate, anti-parasitic compound PHMB, and various antiglaucoma drugs.<sup>35–41</sup> In our previous transcorneal experiments, we observed up to 10 drug delivery enhancements with minimal and reversible changes in the eye tissues, as determined in short-term safety studies. Few studies have been conducted using therapeutic ultrasound to enhance sclera drug delivery. The most significant factors of therapeutic ultrasound in enhancing drug delivery are cavitation and acoustic streaming effects.<sup>37,40,42</sup> A study of ultrasound-mediated transscleral delivery of macromolecules showed that low frequency and low-intensity ultrasound (40 kHz at 0.12 W/cm<sup>2</sup>) had significantly enhanced the transscleral penetration of fluorescent dextran (70 kDa) by 1.48 times in *in vivo* rabbit model.<sup>43</sup> Higher frequency low-intensity ultrasound application (1 MHz at 0.05 W/cm<sup>2</sup>) also resulted in permeability increase of fluorescein isothiocyanate diffusion through the sclera.<sup>44</sup> A study of Fluorescent dextran of different sizes (20–150 kDa) with ultrasound frequency (40 kHz–3 MHz) at 0.05 W/cm<sup>2</sup> on fresh rabbit sclera *ex vivo* found the ultrasound application increased sclera penetration up to 20 fold for molecules  $\leq 70$  kDa and up to 3 fold for  $\geq 70$  kDa molecules.<sup>45</sup> Further, a commercial ultrasound drug delivery system - SonoEye with proprietary ultrasound parameters (Seagull Technology, Sydney, Australia) showed successful transscleral delivery of Avastin to the posterior segment of *in vivo* rabbit eye models.<sup>46</sup> *In vitro* studies of isolated human sclera showed a 7.5 enhancement in Avastin sclera delivery using iontophoretic technique.<sup>47</sup> However, *in vitro* transscleral studies also showed that Avastin has low transscleral permeability and long lag time for its molecular size and hindered diffusion (with Avastin reported lag time of  $24 \pm 13$  hours, mean  $\pm$  standard deviation).<sup>7</sup> Ultrasound frequency is inversely proportional to the cavitation effects that are a factor in enhancing drug delivery.<sup>37,40,41</sup> In our study, the ultrasound parameters used were in the medium range to generate cavitation to enhance scleral permeability while ensuring thermal safety.<sup>37,40–42,48</sup>

Our goal was to determine whether therapeutic ultrasound can offer an alternative minimally invasive method for the delivery of macromolecules to different regions of the eye via the transscleral route. Specifically, the main objective of our research was to test the efficacy and safety of ultrasound delivery of the macromolecule Avastin through the sclera in vitro using a standard diffusion cell model.

## Materials and Methods

Bevacizumab (4 mL) bottles (Avastin; Besse Medical, Township, OH, USA) were purchased at a concentration of 100 mg/4 mL (25 mg/mL). Avastin was chosen as a representative of a multitude of different macromolecules for use in the treatment of retinal diseases.<sup>49,50</sup> Avastin bottles were stored in the refrigerator at 4°C. Healthy adult New Zealand white rabbit eyes were purchased from Pel-Freez Biologicals (Rogers, AR, USA). In ophthalmic research, rabbit eyes are the standard model for the human eye.<sup>44</sup> The rabbit eye diameter is 6.5 mm smaller than the average human eye.<sup>51</sup> Rabbit cornea and sclera are 0.25 and 0.42 mm thinner than in human, respectively.<sup>51,52</sup> The rabbit eyes were harvested immediately after euthanization, stored in Dulbecco's modified Eagle's medium (DMEM), and shipped overnight on ice. Before use, the rabbit eyes were visually examined to remove the eyes with scleral damage. Dulbecco phosphate-buffered saline (DPBS, D4031; Millipore Sigma, Burlington, MA, USA) was placed in a water bath at 34.6°C for no longer than 20 minutes prior to the experiment. Rabbit eye samples (consisting of

conjunctiva, sclera, choroid, and retina) were dissected and stored in DPBS at room temperature for <10 minutes before therapeutic ultrasound experiments.

Jacketed Franz diffusion cells (PermeGear, Hellertown, PA, USA) were used in our experiments as they represent a standard in vitro drug delivery testing system (Fig. 1A). The orifice diameter is 9 mm, and the volumes of the donor and receiver compartments are 25 and 5 mL, respectively. The receiver compartment was filled with 5 mL of DPBS with a magnetic stir bar. The dissected rabbit sclera was placed in the center of the diffusion cell and clamped with the episcleral layer facing the donor compartment. The donor compartment was filled with Avastin solution. The diffusion cells were placed in an immersion circulator water bath at 34.6°C and stirred at 380 rpm (see Fig. 1B). The water bath temperature was chosen to mimic the eye surface temperature of  $34.5 \pm 0.8^\circ\text{C}$ .<sup>53</sup>

After 60 minutes, the sclera and surrounding eye layers were collected in a glass container with 10% neutral buffered formalin (Fisher Scientific, Waltham, MA, USA) for histological studies (Histoserv Inc., Germantown, MD, USA). Structural changes in the hematoxylin and eosin (H&E) stained sections (consisting of conjunctiva, sclera, choroid, and retina) were performed using an upright ZeissAxio Imager (Carl Zeiss Inc., Jena, Germany). The 1  $\mu\text{m}$  thick sclera sections were imaged with a 40X/0.65 NA air objective (A-Plan, Carl Zeiss Inc., Jena, Germany). Observations were utilized to determine potential changes in the eye tissue structure due to ultrasound application. The receiver compartment solution was collected with a glass pipette, and the absorbance was measured with a SpectraMax QuickDrop

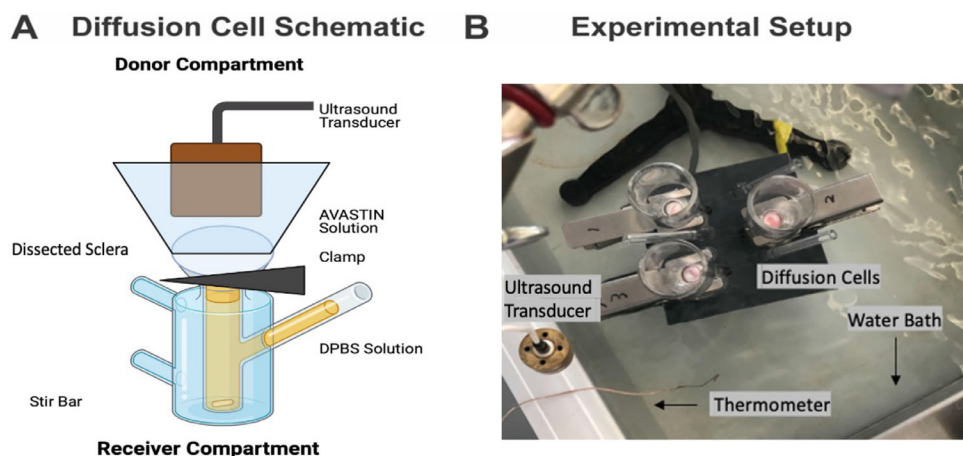


**Figure 1.** Experimental configuration. (A) Diffusion cell schematic. The donor compartment is filled with Avastin solution, and the receiver compartment with DPBS. Sclera is placed as a barrier between the two compartments. The ultrasound transducer is placed in the donor compartment. Created with [BioRender.com](https://www.biorender.com). (B) Experimental setup. Three diffusion cells were placed inside a temperature-controlled water bath at 34.6°C. The ultrasound transducer was removed from the donor compartment after ultrasound application.

micro-volume spectrophotometer (Molecular Devices, San Jose, CA, USA) to measure the absorbance differences between the ultrasound- and sham-treatment groups. The peak of Avastin absorbance was reported previously at 280 nm.<sup>54</sup> The unpaired *t*-test assuming unequal variances was used to compare the receiver compartment absorbance distribution of the sham and ultrasound groups.<sup>35–37,39–41,55</sup>

The background absorbance is the absorbance of the receiver compartment after an experiment in which the donor and receiver compartments have only saline buffer. This background absorbance was present in our previous in vitro diffusion cell studies and was believed to be due to diffusion of biological compounds from the eye tissues into the receiver compartment.<sup>39</sup> The calibrated mean was calculated by subtracting the mean of the background absorbance from the mean of the measured drug absorbance.

The calibrated standard deviation for the sham-treated and ultrasound-treated groups was calculated using the following formula:

$$SD_{E, \text{Calibrated}} = \frac{SD_{E, \text{Measured}} + SD_{E, \text{Background}} - (2 \times \text{Corr} \times SD_{E, \text{Measured}} \times SD_{E, \text{Background}})}{\sqrt{SD_{E, \text{Measured}}^2 + SD_{E, \text{Background}}^2 - (2 \times \text{Corr} \times SD_{E, \text{Measured}} \times SD_{E, \text{Background}})}}$$

where the “ $SD_{E, \text{Calibrated}}$ ” is the SD of the difference scores, and the “ $SD_{E, \text{Measured}}$ ” and “ $SD_{E, \text{Background}}$ ” are the measured drug absorbance and background absorbance, respectively. “Corr” is the Pearson correlation between drug absorbance and background absorbance and is expected to be zero in our experiments, as these measurements were performed in the separate sets of experiments.<sup>56</sup>

The calibration curve of absorbance versus Avastin concentration was measured at 280 nm using a Spectra-Max QuickDrop micro-volume spectrophotometer. The absorbance maximum was detected at 280 nm.<sup>54</sup> The spectrophotometer was used to measure the absorbance of solutions of known Avastin concentration. The concentration of Avastin was calculated using the following formula:

$$Y = 1.1024 \times X$$

where Y is the absorbance value at 280 nm and X is the drug concentration in the sample ( $\mu\text{g/mL}$ ). The  $R^2$  value of the calibration curve was 0.91.

### The 400 kHz Ultrasound Application

Two milliliters of the drug solution (Avastin) were used to fill the donor compartment, after placing the 400 kHz ultrasound transducer at the desired distance with an intensity of  $1 \text{ W/cm}^2$ . For optimal energy delivery, the transducer was placed and located at

the near-field to the far-field distance from the sclera ( $d_{ff}$ ) at 1.0 cm as it is the location for the furthest maximum pressure of the 400 kHz unfocused transducer.<sup>36</sup> Unfocused, custom-designed circular transducers (Sonic Concepts, Bothell, WA, USA) with a 15 mm active diameter were used for therapeutic ultrasound working at 400 kHz were utilized in these experiments.<sup>57</sup>

The ultrasound intensity at different input settings was measured using a reflective radiation force balance with an ultrasound power meter (Ohmic Instruments, St. Charles, MO, USA). The driving unit consisted of a function generator (33250; Agilent, Santa Clara, CA, USA) and a power amplifier (150A100B; Amplifier Research, Souderton, PA, USA) connected to the ultrasound transducer by an electrical power meter (Sonic Concepts, Bothell, WA, USA). Sham treatment (no ultrasound) or ultrasound was applied for 5 minutes in the sham and ultrasound groups, respectively. In a previous modeling study, 5.5 minutes of ultrasound treatment time was observed to be the length of time for the human eye model to reach the desired cumulative drug concentration.<sup>58</sup> The ultrasound transducer was then removed, and the rabbit sclera was incubated for 55 minutes in the water bath at  $34.6^\circ\text{C}$ . A total of 60 minutes of drug exposure was applied for both ultrasound- and sham-treated cases; however, ultrasound-treated samples were first exposed to ultrasound for 5 minutes at the beginning of drug exposure. A schematic of the timeline of the experimental procedure is shown in Figure 2.

The temperature of the donor compartment was measured immediately before applying the ultrasound (0 minutes), and 2.5 and 5 minutes after the start of ultrasound application. The data sets were as follows: no ultrasound (sham)  $n = 15$ , and ultrasound (400 kHz)  $n = 17$ . Outliers were removed in each of the sham and ultrasound-treated experiments using the MATLAB outlier removal function. The data sets without outliers had the following number of data points: no ultrasound (sham)  $n = 13$ , and ultrasound (400 kHz)  $n = 15$ . The background absorbance values of the receiver compartment were  $0.004 \pm 0.001$  ( $n = 3$ ) for the sham group and  $0.013 \pm 0.004$  ( $n = 3$ ) for the ultrasound group.

### The 3 MHz Ultrasound Application

One milliliter of Avastin filled the donor compartment in both the 3 MHz ultrasound and sham treatment groups. Ultrasound was applied at a frequency of 3 MHz and an intensity of  $1 \text{ W/cm}^2$ . The transducer was placed 5 mm from the sclera ( $d_{ff}$ ). The receiver compartment was stirred at 380 rpm using a 3 mm

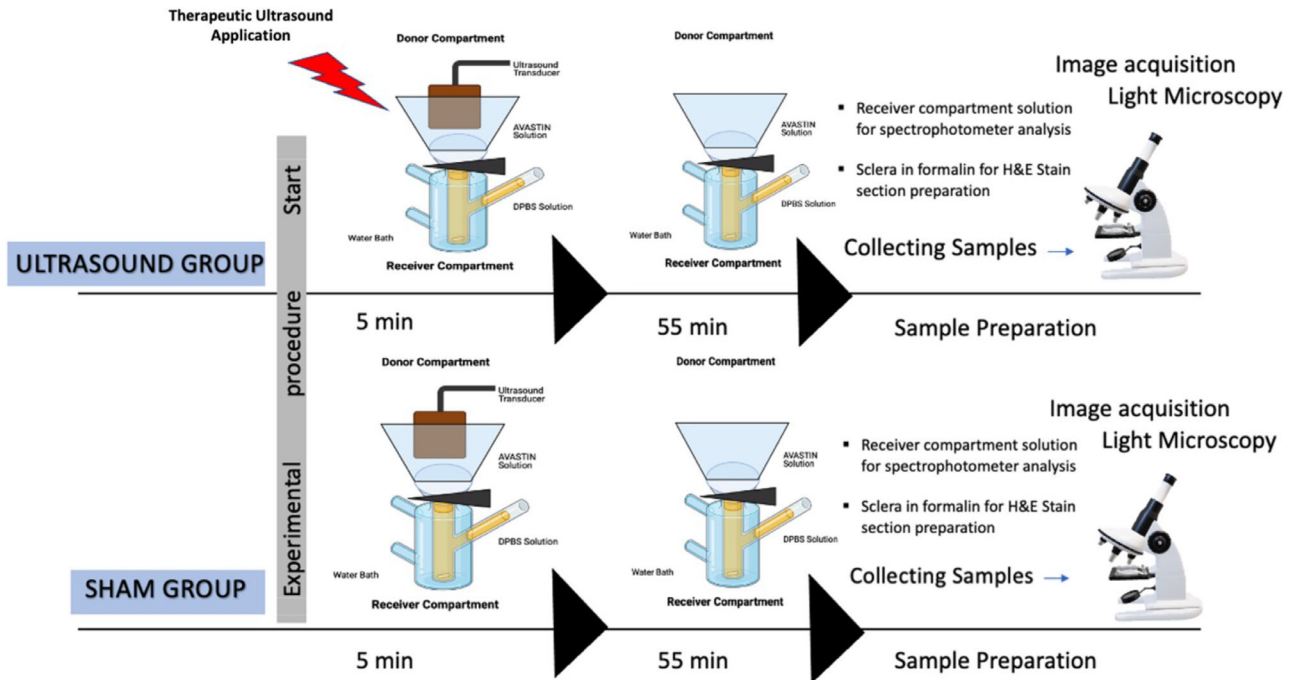


**Figure 2.** A schematic showing the timeline of the experimental procedure in ultrasound and sham treatments. Created with BioRender.com.

magnetic stir bar. A protocol step that included rinsing of the dissected eye tissue two to three times with DPBS wash before the experiments, was added to the 3 MHz experiments to minimize the potential diffusion of biological compounds from the sclera into the receiver compartment.<sup>39</sup> The diffusion cell was placed in the immersion circulator at 34.6°C, as described previously. A portable physiotherapy ultrasound device with an ultrasound transducer with an active diameter of 10 mm (3.3 MHz) was used (Sonicator 740; Mettler Electronics, Anaheim, CA, USA). The transducer spatial pattern is a collimated (cylindrical) beam with an effective radiating area of 1 cm<sup>2</sup>, measured from 5 mm from the ceramic surface disc of the transducer.<sup>57</sup> The donor compartment temperatures were measured before and after ultrasound treatment application for the 3 MHz ultrasound-treated group, or for the sham-treated group but without turning the ultrasound on. The data set had the following number of data points: no ultrasound (sham)  $n = 7$ , and ultrasound (3 MHz)  $n = 8$ . Background absorbance values of the receiver compartment were for 0.0 ( $n = 2$ ) for the sham group and 3 MHz ultrasound group 0.0 ( $n = 1$ ).

### Histological Analysis

Sclera is a dense connective tissue composed of collagen fibers and divided into four layers: episclera, stroma, lamina fusca, and endothelium.<sup>59</sup> Histological observations for scleral damage were adopted as

the modified method for corneal damage described in Nabili et al. 2014. Briefly, different classes of scleral damage were defined as follows: Class 1 (no damage): the four scleral layers are discernible as episclera, stroma, lamina fusca, and endothelium. Cell nuclei were visible in the episclera. Class 2: Four scleral layers were visualized. Episclera layers appear slightly damaged, and the cellular structure is more challenging to observe. The endothelium was intact. Class 3: Only two layers are discernible as episclera and stroma, with more substantial damage observed in the endothelium. Class 4: Scleral tissue is damaged, and layers are not identifiable.<sup>37</sup> Additional histological observations of the sclera samples (negative control,  $n = 3$ ) exposed to 34.6°C bath solution for 60 minutes without the drug and without ultrasound application to identify the potential influence of prolonged drug (Avastin) exposure on the sclera. The negative control ( $n = 3$ ) saline-only exposure was compared to the sham group (with Avastin and no ultrasound exposure) to determine if other factors in addition to ultrasound are damaging the sclera in the water bath.

## Results

Spectrophotometric analysis of the receiver compartment solution at the Avastin maximal

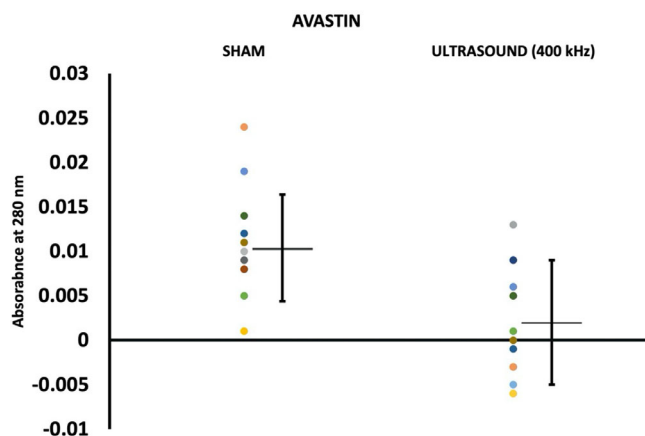


**Figure 3.** Avastin absorbance measurements. No ultrasound (sham;  $n = 13$ ) and 400 kHz ultrasound Groups ( $n = 15$ ). Background absorbance of solvent was subtracted from measurements. No statistical difference was observed between sham and 400 kHz ultrasound groups. The horizontal lines are the calibrated mean and error bars are the standard deviation ( $SD_{E, \text{Calibrated}}$ ).

absorbance of 280 nm indicated that there was no statistical difference ( $P > 0.05$ , unpaired  $t$ -test) between the sham group and the 400 kHz ultrasound treated group (Fig. 3). The absorbance values were  $0.014 \pm 0.007$  ( $n = 13$ ) in the sham group and  $0.015 \pm 0.006$  ( $n = 15$ ) in the ultrasound group, with no statistical difference. The calibrated absorbance values for the sham and 400 kHz ultrasound groups were  $0.010 \pm 0.006$  and  $0.002 \pm 0.007$ , respectively. The average temperatures were  $26.7^\circ\text{C}$ ,  $29.7^\circ\text{C}$ , and  $30.5^\circ\text{C}$  ( $n = 5$ ) in the sham group, and  $27.9^\circ\text{C}$ ,  $38.4^\circ\text{C}$ , and  $46.5^\circ\text{C}$  ( $n = 8$ ) in the ultrasound group at 0, 2.5, and 5 minutes, respectively. The average concentration values for the sham group were  $0.013 \pm 0.005$  ( $\mu\text{g/mL}$ ) and  $0.013 \pm 0.005$  ( $\mu\text{g/mL}$ ) for the 400 kHz ultrasound group.

To verify therapeutic ultrasound safety in scleral tissues in vitro, H&E-stained scleral sections were

imaged to identify structural changes and damage. Histological imaging showed no changes in the surface of the sclera due to exposure to 400 kHz ultrasound. Histological images of the sham and 400 kHz ultrasound treated sclera are shown in Figure 4. Histological observations for scleral damages that were adopted from Nabili et al. 2014 showed that both groups had structural changes in the surface of the episclera in the 400 kHz ultrasound and sham group, whereas application of 400 kHz ultrasound produced slightly more endothelial damage (Table 1). The temperature of the donor compartment was measured immediately before applying the ultrasound, and 2.5 and 5 minutes after the start of 400 kHz ultrasound application. The average temperature was  $26.7 \pm 1.7^\circ\text{C}$ ,  $29.7 \pm 2.7^\circ\text{C}$ ,  $30.5 \pm 1.6^\circ\text{C}$ , and  $27.9 \pm 1.2^\circ\text{C}$ ,  $38.4 \pm 4.9^\circ\text{C}$ ,  $46.5 \pm 3.9^\circ\text{C}$  in the sham group ( $n = 5$ ) and the ultrasound group ( $n = 8$ ) at 0, 2.5, and 5 minutes, respectively.

Spectrophotometric measurements of the receiver compartment solution at the Avastin maximal absorbance of 280 nm indicated a statistical difference ( $P < 0.01$ , unpaired  $t$ -test) between the sham group  $0.002 \pm 0.0005$  ( $n = 7$ ) and the 3 MHz ultrasound treated groups  $0.004 \pm 0.0019$  ( $n = 8$ ; Fig. 5). There was a 2.3 times increase in drug delivery in the 3 MHz ultrasound group when compared to the corresponding sham group. The average concentration values for the sham group were  $0.001 \pm 0.0005$  ( $\mu\text{g/mL}$ ) and  $0.004 \pm 0.001$  ( $\mu\text{g/mL}$ ) for the 3 MHz ultrasound group. The difference in the absorbance reading of the two aforementioned sham groups may be due to the scleral DPBS wash prior to the experiment that was added to the 3 MHz ultrasound group. The donor compartment temperatures were measured before and after ultrasound treatment application for the 3 MHz ultrasound-treated group and its sham-treated group. The average temperatures were  $24.1 \pm 2.2^\circ\text{C}$  and

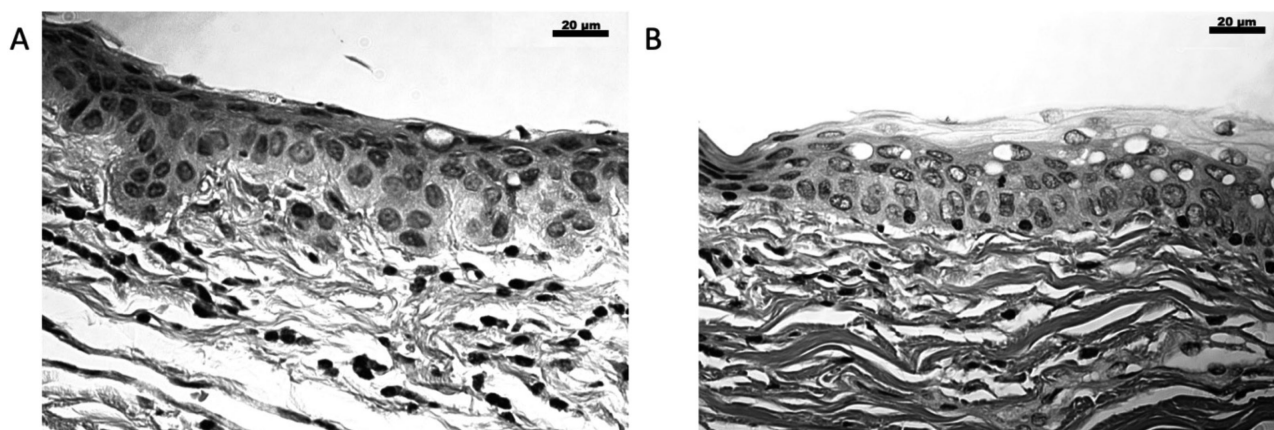


**Figure 4.** Sclera 40X objective images under light microscope. (A) Sham group. (B) 400 kHz ultrasound group. The bar scale is 20  $\mu\text{m}$ .

**Table 1.** Classification of Scleral Structural Changes in the Sham and 400 kHz Ultrasound Groups

Group	Class 1	Class 2	Class 3	Class 4	Total
Sham no ultrasound	4	8	2	1	15
Ultrasound 400 kHz and 1.0 W/cm <sup>2</sup>	6	5	6	1	18

**Class 1 (no damage):** The four scleral layers are discernible as episclera, stroma, lamina fusca, and endothelium. Cell nuclei were visible in the episclera. **Class 2:** Four scleral layers were visualized. Episclera layers appear slightly damaged, and the cellular structure is more challenging to observe. The endothelium was intact. **Class 3:** Only two layers are discernible as episclera and stroma, with more substantial damage observed in the endothelium. **Class 4:** Scleral tissue is damaged, and layers are not identifiable.

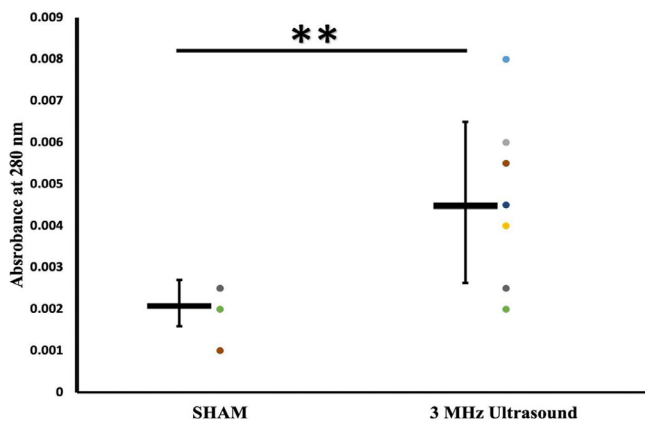


**Figure 5.** Absorbance measurement of 3 MHz ultrasound ( $n = 8$ ) and sham group ( $n = 7$ ) at 280 nm. The horizontal line is the mean and the error bar is the Standard Deviation (SD). \*\*Statistical significance level  $<0.01$ .

$27.28 \pm 1.0^{\circ}\text{C}$  ( $n = 5$ ) for the sham-treated group, and  $26.1 \pm 1.9^{\circ}\text{C}$  and  $28.3 \pm 0.4^{\circ}\text{C}$  ( $n = 4$ ) for a 3 MHz ultrasound-treated group at 0 minutes and 5 minutes after the start of the treatment.

Histology imaging showed structural changes in the surface of the episclera in the 3 MHz ultrasound and sham groups, while application of 3 MHz ultrasound produced more endothelial damage than the sham group (Table 2). Histological images of the sham (left) and 3 MHz ultrasound (right)-treated sclera are shown in Figure 6. The negative control in comparison to sham groups was analyzed to identify the poten-

tial influence of prolonged drug (Avastin) exposure. Our histological data indicate that prolonged Avastin exposure did not damage the sclera (Fig. 7). No statistical difference between the negative control and sham groups was identified in the histological observation adopted from Nabili et al. 2014.

## Discussion

A previous study showed no presence of anti-VEGF (Avastin) in the aqueous or/and vitreous solution after topical application in human eyes.<sup>60</sup> Although anti-VEGF injections are effective, ophthalmologists have noticed the problem of patient noncompliance with monthly therapy visits.<sup>30,34</sup> The use of ultrasound to enhance anti-VEGF drug delivery may result in better patient outcomes in terms of treatment compliance and the avoidance of injection-related adverse effects.<sup>31</sup> Therefore, as opposed to our previous studies indicating the effectiveness of ultrasound in enhancing drug delivery through the cornea, our preliminary results suggest that ultrasound at 400 kHz parameters may not be effective in the delivery of Avastin through the sclera. In comparison, in vitro studies utilizing 400 and 600 kHz ultrasound at intensities of 0.8 at 1.0 W/cm<sup>2</sup>, respectively, yielded a twofold increase in the permeation of dexamethasone, an anti-inflammatory drug through the cornea.<sup>36</sup> Further, in vivo experimentation of DEX in rabbits showed a statistically signifi-

**Table 2.** Classification of Scleral Structural Changes in the Sham and 3 MHz Ultrasound Groups

Group	Class 1	Class 2	Class 3	Class 4	Total
Sham no ultrasound	0	1	2	3	6
Ultrasound 3 MHz and 1.0 W/cm <sup>2</sup>	0	0	5	1	6

**Class 1 (no damage):** The four scleral layers are discernible as episclera, stroma, lamina fusca, and endothelium. Cell nuclei were visible in the episclera. **Class 2:** Four scleral layers were visualized. Episclera layers appear slightly damaged, and the cellular structure is more challenging to observe. The endothelium was intact. **Class 3:** Only two layers are discernible as episclera and stroma, with more substantial damage observed in the endothelium. **Class 4:** Scleral tissue is damaged, and layers are not identifiable.

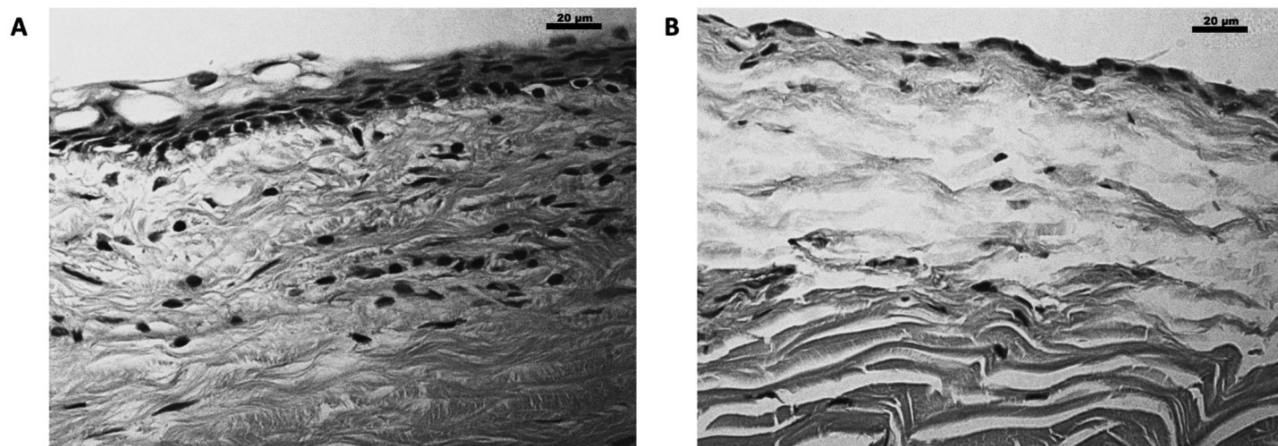


**Figure 6.** Sclera 40X objective images under light microscope. (A) Sham group. (B) 3 MHz ultrasound group. The bar scale is 20 μm.

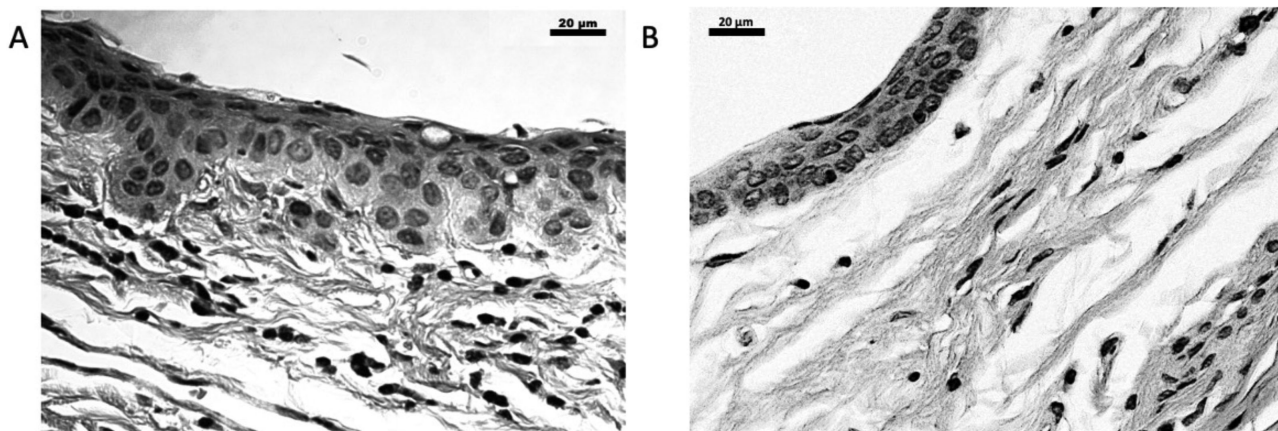


**Figure 7.** Sclera 40X objective images under light microscope. (A) Sham group. (B) Saline only (negative control). The bar scale is 20 μm.

cant 2.8 and 2.4 increase in the amount of drug in the aqueous humor of 400 and 600 kHz ultrasound-treated corneas as compared to sham corneas, respectively.<sup>37</sup> Sclera might not be the only barrier involved. Other static barriers, such as the retinal pigment epithelium, conjunctiva, and dynamic barriers, such as choroidal blood flow and orbital clearance, should be considered and taken into account in future in vivo experiments.<sup>5</sup> Using higher frequency ultrasound at 3 MHz enhanced the scleral permeability to Avastin, possibly by enhancing ultrasound streaming effects.<sup>45</sup> Transdermal ultrasound studies using frequencies of 1 to 3 MHz showed that cavitation is the major mechanism of enhancing the skin permeability.<sup>61</sup> Our preliminary results provide support that ultrasound at 3 MHz and 1 W/cm<sup>2</sup> may be effective in the delivery of Avastin through the sclera as compared to 400 kHz ultrasound application and sham treatment. A higher frequency ultrasound application (1 MHz at 0.05 W/cm<sup>2</sup>) also resulted in increased permeability of protein diffusion through

the sclera in previously published studies.<sup>44</sup> Potential ultrasound effect on sclera structure was minimal at 400 kHz when compared to their matched sham group. Histological observations for scleral damage indicated that there was no significant difference between the 400 kHz group and their matched sham group. In fact, the recorded damage in both the ultrasound and sham groups indicates that some of the damage may not be the result of ultrasound effects on the tissues, yet due to sample processing and/or during sample collection. Histological observations of scleral damages in the 3 MHz ultrasound and its corresponding sham group showed similar layers of episcleral damage, but the ultrasound group had more endothelial damage.

The maximum scleral temperature change for 400 kHz ultrasound application was 26.9°C ( $n = 8$ ), which was estimated to be mostly due to the heat dissipation of the ultrasound transducer into a small volume of the donor compartment. The maximum

scleral temperature exposure reached 54.1°C after 5 minutes of 400 kHz ultrasound application, which is lower than the threshold temperature for thermal damage in the sclera of 60°C for 10 minutes<sup>62</sup>; therefore functional changes due to heat are unlikely. The maximum scleral temperature change was 4.4°C ( $n = 4$ ) for 3 MHz ultrasound application, and there appeared to be no significant heat dissipation from the transducer as a self-heat artifact.<sup>63</sup> The average sclera temperature rise was 2.2 and 18.6°C for 3 MHz ( $n = 4$ ) and 400 kHz ( $n = 8$ ), respectively. The 400 kHz transducer was less efficient than the 3 MHz transducer which results in more heating.<sup>63</sup> In potential clinical treatment, the temperature elevation could be corrected by better transducer manufacturing methods and/or cooling treatment on the sclera surface to minimize the thermal increase. Moreover, the pulsing mode of ultrasound application results in a lower temperature increase than the continuous mode, and this approach could also be utilized to minimize the thermal effects.<sup>64</sup> The US Food and Drug Administration (FDA) and World Federation for Ultrasound in Medicine and Biology set a 1.0°C thermal index limit for all ocular applications because of the sensitivity of the eye lens to the higher temperature; however, the index limit is for diagnostic application.<sup>65</sup>

Intravitreal injection of Avastin requires a monthly injection, which may lead to discomfort, infections, and other complications.<sup>20–22</sup> Using therapeutic ultrasound to deliver Avastin into the eye could eliminate these risks and may allow for drug delivery with fewer complications.<sup>45</sup> Our minimally invasive technology shows promise for delivering macromolecules into the eye. The proposed technology may be helpful in delivering anti-VEGF agents for patients with diabetic eye-related diseases, such as diabetic retinopathy.<sup>17,18</sup> Diabetic retinopathies can be screened, diagnosed, and monitored using different imaging modalities, such as color fundus photography, B-scan ultrasonography, FA, and optical coherence tomography (OCT).<sup>66–68</sup> Biomarkers could also be considered before and after the treatment decision in patients with DME for significant functional and anatomical improvements.<sup>69,70</sup> Future clinical studies should incorporate imaging methods by visualizing the peripheral retina using ultra-widefield fluorescein angiography (UWFA) and/or spectral domain optical coherence tomography (SD-OCT) to validate our treatment effectiveness.<sup>25,66,68,71,72</sup> A study showed that detectable features on OCT with detailed examination biomicroscopy can distinguish optic disc pit maculopathy (ODPM) that would help avoid underdiagnosis.<sup>73</sup> If successful, our proposed technology may lead to a change in the standard of care and may lessen post-

surgery complications and increase patient compliance.<sup>31</sup> The proposed technology has the potential to change the delivery procedures for anti-VEGF drugs. The proposed ultrasound application is not expected to significantly change the daily clinical protocols of a retina specialist; however, it may make the whole process easier for patients with fewer complications afterwards. Although outside of the scope of the current study, it would be important to test the effectiveness of ultrasound in enhancing delivery of a range of macromolecules used in the treatment of retinopathies, including direct comparison of bevacizumab (Avastin) with a molecular weight of 149 kDa with ranibizumab and aflibercept, which have molecular weights of 48 and 115 kDa, respectively.<sup>34,74</sup> Modeling of ultrasound application in a pulsed and continuous mode would allow for further understanding of the thermal changes in different eye tissues during ultrasound application. In future studies, we plan to test this technology in long-term animal studies *in vivo* and in subsequent clinical trials. Further studies should also incorporate different ranges of ultrasound frequencies to test their impact on scleral permeability of Avastin. This study focuses on the application of therapeutic ultrasound to improve topical ocular delivery of macromolecules. The proposed research may address an important clinical problem because there are currently no minimally invasive methods for the delivery of macromolecular drugs to diseased sites for the treatment of retinopathies and other vision-threatening diseases.

## Acknowledgments

The authors thank Papa Lab (The George Washington University, Department of Biomedical Engineering) for their guidance on the absorbance measurement.

Funded by The Foundation for Prevention of Blindness Society of Metropolitan Washington awarded to our collaborator Fadi Nasrallah as the principal investigator (PI) and Zderic as a co-PI.

**Conflict of Interest Statement:** The authors certify that they have no affiliations with or involvement in any organization or entity with any financial interest or nonfinancial interest in the subject matter or materials discussed in this manuscript.

**Disclosure:** H.H. Almogbil, None; F.P. Nasrallah, None; V. Zderic, None

## References

- Short BG. Safety evaluation of ocular drug delivery formulations: techniques and practical considerations. *Toxicol Pathol.* 2008;36:49–62.
- Kompella UB, Kadam RS, Lee VHL. Recent advances in ophthalmic drug delivery. *Ther Deliv.* 2011;1:435–456.
- Molokhia SA, Thomas SC, Garff KJ, Mandell KJ, Wirostko BM. Anterior eye segment drug delivery systems: Current treatments and future challenges. *J Ocul Pharmacol Ther.* 2013;29:92–105.
- Kim YC, Chiang B, Wu X, Prausnitz MR. Ocular delivery of macromolecules. *J Control Release.* 2014;190:172–181.
- Agrahari V, Mandal A, Agrahari V, et al. A comprehensive insight on ocular pharmacokinetics. *Drug Deliv Transl Res.* 2016;6:735–754.
- Suri R, Beg S, Kohli K. Target strategies for drug delivery bypassing ocular barriers. *J Drug Deliv Sci Technol.* 2019;55:101389.
- Wen H, Hao J, Li SK. Characterization of human sclera barrier properties for transscleral delivery of bevacizumab and ranibizumab. *J Pharm Sci.* 2013;102(3):892–903.
- Demetriades AM, Deering T, Liu H, et al. Transscleral delivery of antiangiogenic proteins. *J Ocul Pharmacol Ther.* 2008;24(1):70–79.
- Olsen TW, Edelhauser HF, Lim JI, Geroski DH. Human scleral permeability. Effects of age, cryotherapy, transscleral diode laser, and surgical thinning. *Invest Ophthalmol Vis Sci.* 1995;36(9):1893–1903.
- Ambati J, Canakis CS, Miller JW, et al. Diffusion of high molecular weight compounds through sclera. *Invest Ophthalmol Vis Sci.* 2000;41(5):1181–1185.
- Gaudana R, Ananthula HK, Parenky A, Mitra AK. Ocular drug delivery. *AAPS J.* 2010;12:348–360.
- Kim HM, Han H, Hong HK, et al. Permeability of the Retina and RPE-Choroid-Sclera to Three Ophthalmic Drugs and the Associated Factors. *Pharmaceutics.* 2021;13(5):655.
- Joseph M, Trinh HM, Cholkar K, Pal D, Mitra AK. Recent perspectives on the delivery of biologics to back of the eye. Expert Opinion on Drug Delivery. *Taylor and Francis Ltd.* 2017;14:631–645.
- Patel A, Cholkar K, Agrahari V, Mitra AK. Ocular drug delivery systems: An overview. *World J Pharmacol.* 2013;2(2):47–64.
- Gaudana R., Jwala J., Boddu S. H., Mitra A. K. Recent perspectives in ocular drug delivery. *Pharm Res.* 2009;26(5):1197–1216.
- Irimia T, Ghica MV, Popa L, Anuța V, Arsene AL, Dinu-Pirvu CE. Strategies for improving ocular drug bioavailability and corneal wound healing with chitosan-based delivery systems. *Polymers.* 2018;10:1221.
- Cohen MH, Gootenberg J, Keegan P, Pazdur R. FDA Drug Approval Summary: Bevacizumab (Avastin) Plus Carboplatin and Paclitaxel as First-Line Treatment of Advanced/Metastatic Recurrent Nonsquamous Non-Small Cell Lung Cancer. *Oncologist.* 2007;12(6):713–718.
- Kazazi-Hyseni F, Beijnen JH, Schellens JHM. Bevacizumab. *Oncologist.* 2010;15(8):819–825.
- Wallsh JO, Gallemore RP. Anti-VEGF-Resistant Retinal Diseases: A Review of the Latest Treatment Options. *Cells.* 2021;10(5):1049.
- Falavarjani KG, Nguyen QD. Adverse events and complications associated with intravitreal injection of anti-VEGF agents: a review of literature. *Eye (Lond).* 2013;27(7):787–794.
- Shikari H, Silva PS, Sun JK. Complications of intravitreal injections in patients with diabetes. *Semin Ophthalmol.* 2014;29(5-6):276–289.
- Shin SH, Park SP, Kim YK. Factors Associated with Pain Following Intravitreal Injections. *Korean J Ophthalmol.* 2018;32(3):196–203.
- Iglicki M, Zur D, Busch C, Okada M, Loewenstein A. Progression of diabetic retinopathy severity after treatment with dexamethasone implant: a 24-month cohort study the ‘DR-Pro-DEX Study’. *Acta Diabetol.* 2018;55(6):541–547.
- Iglicki M, González DP, Loewenstein A, Zur D. Next-generation anti-VEGF agents for diabetic macular oedema. *Eye (Lond)*, <https://doi.org/10.1038/s41433-032-01722-8>. [Online ahead of print].
- Iglicki M., Zur D., Fung A., et al. TRAc-tional DIabetic reTInal detachment surgery with co-adjuvant intravitreal DexamethasONE implant: the TRADITION STUDY. *Acta Diabetologica,* 2019;56(10):1141–1147.
- Moon BG, Lee JY, Yu HG, et al. Efficacy and Safety of a Dexamethasone Implant in Patients with Diabetic Macular Edema at Tertiary Centers in Korea. *J Ophthalmol.* 2016;2016:9810270.
- Mello Filho P, Andrade G, Maia A, et al. Effectiveness and Safety of Intravitreal Dexamethasone Implant (Ozurdex) in Patients with Diabetic Macular Edema: A Real-World Experience. *Ophthalmologica.* 2019;241(1):9–16.

28. Zur D, Igllicki M, Loewenstein A. The Role of Steroids in the Management of Diabetic Macular Edema. *Ophthalmic Res.* 2019;62(4):231–236.
29. Mandal A, Pal D, Agrahari V, Trinh HM, Joseph M, Mitra AK. Ocular delivery of proteins and peptides: Challenges and novel formulation approaches. *Advanced Drug Deliv Rev.* 2018; 126:67–95.
30. Mulligan K, Seabury SA, Dugel PU, Blim JF, Goldman DP, Humayun MS. Economic Value of Anti-Vascular Endothelial Growth Factor Treatment for Patients With Wet Age-Related Macular Degeneration in the United States [published correction appears in JAMA Ophthalmol. 2020 Feb 1;138(2):223]. *JAMA Ophthalmol.* 2020;138(1):40–47.
31. Polat O, İnan S, Özcan S, et al. Factors Affecting Compliance to Intravitreal Anti-Vascular Endothelial Growth Factor Therapy in Patients with Age-Related Macular Degeneration. *Turk J Ophthalmol.* 2017;47(4):205–210.
32. Huang D, Wang L, Dong Y, Pan X, Li G, Wu C. A novel technology using transscleral ultrasound to deliver protein loaded nanoparticles. *Eur J Pharm Biopharm.* 2014; 88(1):104–115.
33. Lamy R, Chan E, Zhang H, et al. Ultrasound-enhanced penetration of topical riboflavin into the corneal stroma. *Investig Ophthalmol Vis Sci.* 2013;54(8):5908–5912.
34. Boyer DS, Hopkins JJ, Sorof J, Ehrlich JS. Anti-vascular endothelial growth factor therapy for diabetic macular edema. *Ther Adv Endocrinol Metab.* 2013;4(6):151–169.
35. Karpinecz B, Edwards N, Zderic V. Therapeutic Ultrasound-Enhanced Transcorneal PHMB Delivery In Vitro. *J Ultrasound Med.* 2021;40:2561–2570.
36. Nabili M, Patel H, Mahesh SP, Liu J, Geist C, Zderic V. Ultrasound-enhanced delivery of antibiotics and anti-inflammatory drugs into the eye. *Ultrasound Med Biol.* 2013;39(4):638–646.
37. Nabili M, Shenoy A, Chawla S, et al. Ultrasound-enhanced ocular delivery of dexamethasone sodium phosphate: An in vivo study. *J Ther Ultrasound.* 2014;2(1):6.
38. Nabili M, Geist C, Zderic V. Thermal safety of ultrasound-enhanced ocular drug delivery: A modeling study. *Med Phys.* 2015;42(10):5604–5615.
39. Zderic V, Vaezy S, Martin RW, Clark JI. Ocular drug delivery using 20-kHz ultrasound. *Ultrasound Med Biol.* 2002;28(6):823–829.
40. Zderic V, Clark JI, Vaezy S. Drug delivery into the eye with the use of ultrasound. *J Ultrasound Med.* 2004;23(10):1349–1359.
41. Zderic V, Clark JI, Martin RW, Vaezy S. Ultrasound-enhanced transcorneal drug delivery. *Cornea.* 2004;23(8):804–811.
42. Huang D, Chen YS, Rupenthal ID. Overcoming ocular drug delivery barriers through the use of physical forces. *Advanced Drug Deliv Rev.* 2018;126:96–112.
43. Suen WLL, Wong HS, Yu Y, Lau LCM, Lo ACY, Chau Y. Ultrasound-mediated transscleral delivery of macromolecules to the posterior segment of rabbit eye in vivo. *Investig Ophthalmol Vis Sci.* 2013;54(6):4358–4365.
44. Cheung ACY, Yu Y, Tay D, Wong HS, Ellis-Behnke R, Chau Y. Ultrasound-enhanced intrascleral delivery of protein. *Int J Pharm.* 2010;401(1–2):16–24.
45. Chau Y, Suen WLL, Tse HY, Wong HS. Ultrasound-enhanced penetration through sclera depends on frequency of sonication and size of macromolecules. *Eur J Pharm Sci.* 2017;100:273–279.
46. Zhang H, Yang D, Wigg JP, Unger H, Unger M, Crowston JG. Ultrasound-mediated transscleral delivery of Avastin to the posterior segment of rabbit eye in vivo. *IOVS Annual Meeting Abstract.* 2014;55(13):1804.
47. Pescina S, Ferrari G, Govoni P, et al. In-vitro permeation of bevacizumab through human sclera: effect of iontophoresis application. *J Pharm Pharmacol.* 2010;62(9):1189–1194.
48. Jegal U, Lee JH, Lee J, Jeong H, Kim MJ, Kim KH. Ultrasound-assisted gatifloxacin delivery in mouse cornea, in vivo. *Sci Rep.* 2019;9(1):1–11.
49. Avery RL, Pearlman J, Pieramici DJ, et al. Intravitreal bevacizumab (Avastin) in the treatment of proliferative diabetic retinopathy. *Ophthalmology.* 2006;113(10):1695.
50. Seah I, Zhao X, Lin Q, et al. Use of biomaterials for sustained delivery of anti-VEGF to treat retinal diseases. *Eye.* 2020;34(8):1341–1356.
51. Gwon A. In *Animal Models in Eye Research Panagiotis*, 1st ed., edited by Tsonic A. San Diego, CA: Elsevier; 2008:184–199.
52. Snell R, Lemp M. *Clinical Anatomy of the Eye.* 2nd. England, UK: Blackwell Science, Inc.; 1998.
53. Tkáčová M, Živčák J, Foffová P. A Reference for Human Eye Surface Temperature Measurements in Diagnostic Process of Ophthalmologic Diseases. *MEASUREMENT.* Available at: 2011.
54. Arvinte T, Palais C, Poirier E, et al. Part 1: Physicochemical characterization of bevacizumab in undiluted 25 mg/mL drug product solutions: Comparison of originator with a biosimilar candidate. *J Pharm Biomed Anal.* 2019;175:112742.

55. Almogbil HH, Daszynski C, Rodriguez EA, Singh T, Stepp MA, Zderic V. Therapeutic ultrasound for improving the topical corneal delivery of macromolecules. *J Acoust Soc Am*. 2019;145(3):1894–1895.
56. Cao Y, Singh V, Wang A, et al. Meta-analysis of right ventricular function in patients with aortic stenosis after transfemoral aortic valve replacement or surgical aortic valve replacement. *Ther Adv Chronic Dis*. 2020;11:204062232093377.
57. Christensen DA. *Ultrasonic Bioinstrumentation*. Hoboken, NJ: John Wiley & Sons; 1988.
58. Hariharan P, Nabili M, Guan A, Zderic V, Myers M. Model for porosity changes occurring during ultrasound-enhanced transcorneal drug delivery. *Ultrasound Med Biol*. 2017;43(6):1223–1236.
59. Pradeep T, Mehra D, Le PH. *Histology, Eye*. Treasure Island, FL: StatPearls Publishing; 2019.
60. Moisseiev E, Waisbourd M, Ben-Artzi E, et al. Pharmacokinetics of bevacizumab after topical and intravitreal administration in human eyes. *Graefes Arch Clin Exp Ophthalmol*. 2014;52(2):331–337.
61. Mitragotri S, Blankschtein D, Langer R. Ultrasound-mediated transdermal protein delivery. *Science*. 1995;269(5225):850–853.
62. Rem AI, Oosterhuis JA, Journée-De Korver HG, et al. Temperature dependence of thermal damage to the sclera: Exploring the heat tolerance of the sclera for transscleral thermotherapy. *Exp Eye Res*. 2001;72(2):153–162.
63. Hynynen K, Edwards DK. Temperature measurements during ultrasound hyperthermia. *Med Phys*. 1989;16(4):618–626.
64. Cambier D, D’Herde K, Witvrouw E, Beck M, Soenens S, Vanderstraeten G. Therapeutic ultrasound: temperature increase at different depths by different modes in a human cadaver. *J Rehabil Med*. 2001;33(5):212–215.
65. Palte HD, Gayer S, Arrieta E, et al. Are ultrasound-guided ophthalmic blocks injurious to the eye? a comparative rabbit model study of two ultrasound devices evaluating intraorbital thermal and structural changes. *Anesth Analg*. 2012;115(1):194–201.
66. Rabiolo A, Parravano M, Querques L, et al. Ultra-wide-field fluorescein angiography in diabetic retinopathy: a narrative review. *Clin Ophthalmol*. 2017;11:803–807.
67. Salz DA, Witkin AJ. Imaging in diabetic retinopathy. *Middle East Afr J Ophthalmol*. 2015;22(2):145–150.
68. Gualino V, Tadayoni R, Cohen SY, et al. Optical coherence tomography, fluorescein angiography, and diagnosis of choroidal neovascularization in age-related macular degeneration. *Retina*. 2019;39(9):1664–1671.
69. Zur D, Iglicki M, Sala-Puigdollers A, et al. Disorganization of retinal inner layers as a biomarker in patients with diabetic macular oedema treated with dexamethasone implant. *Acta Ophthalmol*. 2020;98(2):e217–e223.
70. Iglicki M, Lavaque A, Ozimek M, et al. Biomarkers and predictors for functional and anatomic outcomes for small gauge pars plana vitrectomy and peeling of the internal limiting membrane in naïve diabetic macular edema: The VITAL Study. *PLoS One*. 2018;13(7):e0200365.
71. Soliman AZ, Silva PS, Aiello LP, Sun JK. Ultra-wide field retinal imaging in detection, classification, and management of diabetic retinopathy. *Semin Ophthalmol*. 2012;27(5-6):221–227.
72. Lang GE. Optical coherence tomography findings in diabetic retinopathy. *Dev Ophthalmol*. 2007;39:31–47.
73. Iglicki M, Busch C, Loewenstein A, et al. Underdiagnosed optic disk pit maculopathy: Spectral Domain Optical Coherence Tomography Features For Accurate Diagnosis. *Retina*. 2019;39(11):2161–2166.
74. de Sá Quirino-Makarczyk L, Sainz Ugarte M de F, Viana Vieira B, Kniggendorf S, Saito Regatieri CV. Short-term results of early switch from Ranibizumab to Aflibercept in poor or non responder age related macular degeneration in clinical practice. *Int J Retina Vitreous*. 2020;6(1):1–8.